Chemical and Molecular Science

Abderrahman Atifi	Investigation of molecular and interfacial processes of the electrocatalytic conversion of nitrogen to ammonia under ambient conditions using rare earth element and room temperature ionic liquid-based system
Chris Zarzana	Intrinsic Bonding and Reactivity of Actinide Clusters
Corey Efaw	Development, Characterization, and Testing of Solid-State Electrolytes for Batteries
Robert Fox	Investigating the mobility of rare earth element ligand complexes in an electric field

Work supported through the INL Laboratory Directed Research & Development (LDRD) Program under DOE Idaho Operations Office Contract DE-AC07-05ID14517."

Interrogating the Interfacial Processes during Ambient Nitrogen Reduction to Ammonia

PRESENTER:
Abderrahman Atifi

BACKGROUND: Ammonia is a highly desired hydrogen storage and energy carrier medium. Ambient electrochemical conversion of nitrogen to ammonia (e-N_2/NH_3) is a sustainable alternative to the industrial Haber-Bosch, an energy-intensive and non environmental process. Due to low efficiency and production yield, probing the interfacial processes under ambient e-N_2/NH_3 is a major challenge.

METHODS

1. Spectroscopic and DFT study of e-N_2/NH_3
2. Using Attenuated Total Reflection Surface Enhanced Infrared Absorption Spectroscopy

RESULTS

- Conductive BDD features an extended mid-IR and no degradation under electrolysis
- Direct spectroscopic evidence is provided for N_2 reduction to NH_3 and hydrazine

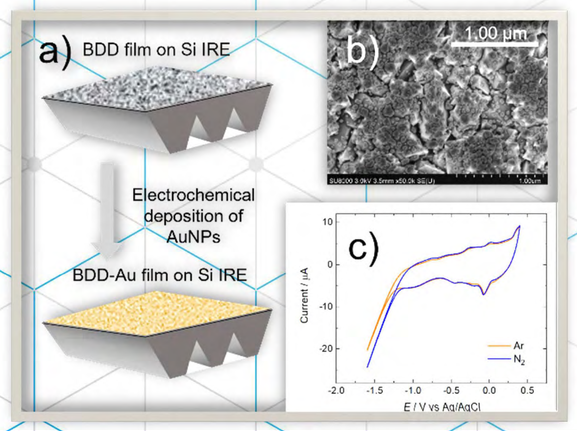

Metal-modified boron-doped diamond with continuous substrate layers provide new opportunities to deploy surface enhanced spectroscopy for interfacial studies under harsh electrocatalytic nitrogen reduction to ammonia conditions

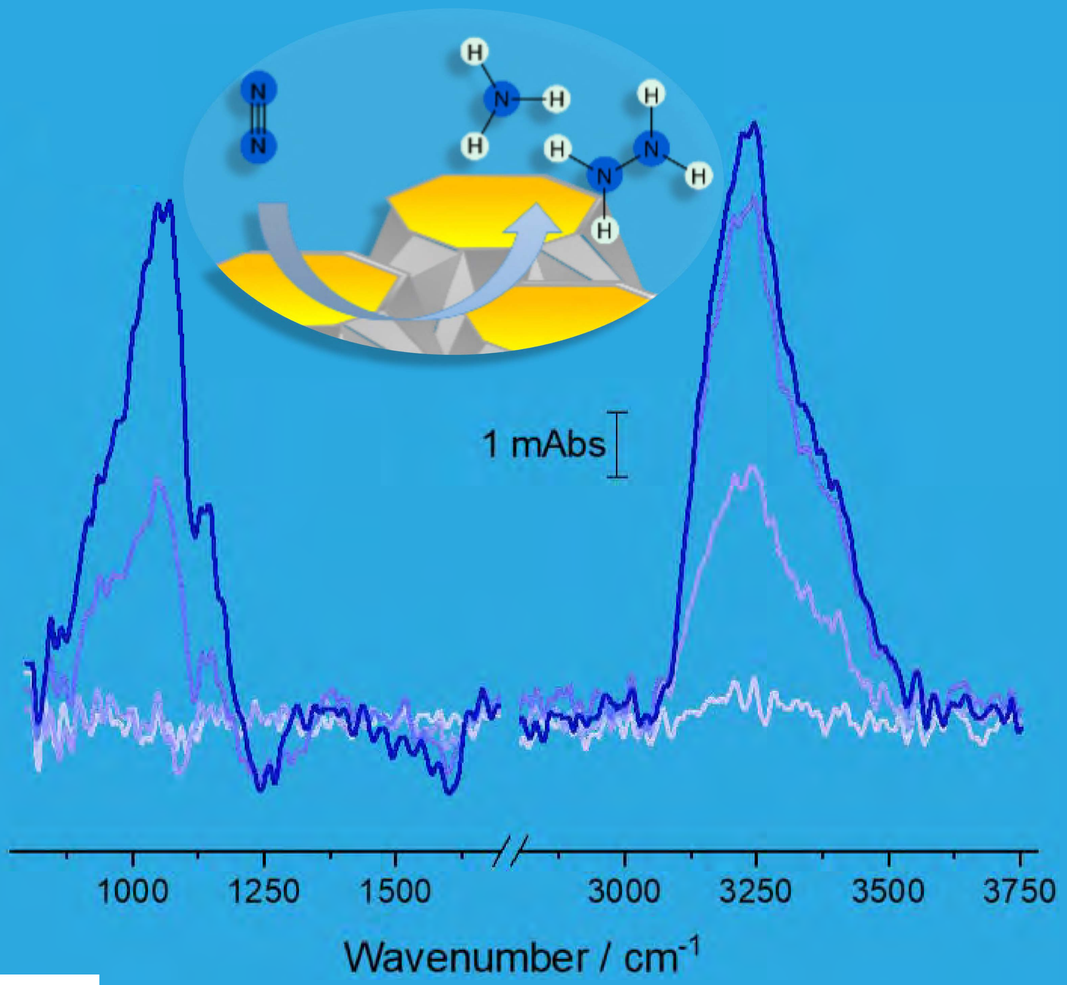

Download the **full paper**

Analytical Chemistry **2023**, 95, 28, 10476−10480

Ionic Liquid Interface under e-N_2/NH_3

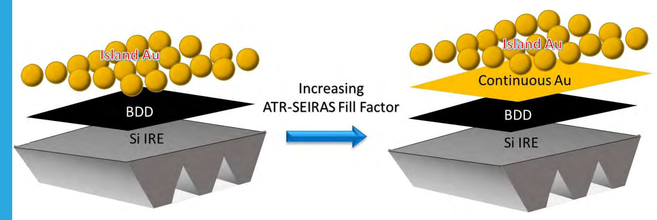

- Continuous Au is key to probe IL interface
- Ionic liquid (IL) is reversibly re-structured under selected potential window
- Irreversible IL interfacial changes under harsh potential conditions may lead to a passivating interface and e-N_2/NH_3 suppression

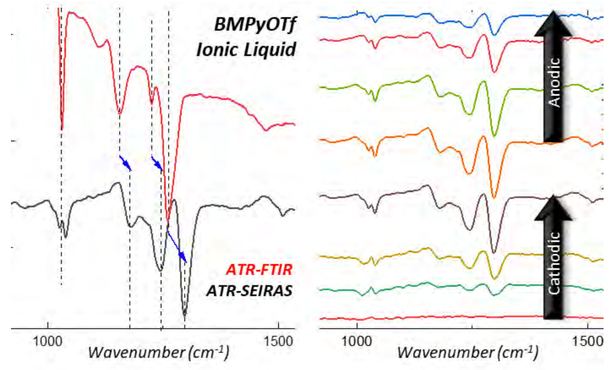

DFT/VASP Calculations

- The IL microstructures at charged Au electrode demonstrate that the applied voltage alters the interfacial arrangement of IL ions
- Fluctuations in the chemical environment at the interface are expected to influence the electrochemical process

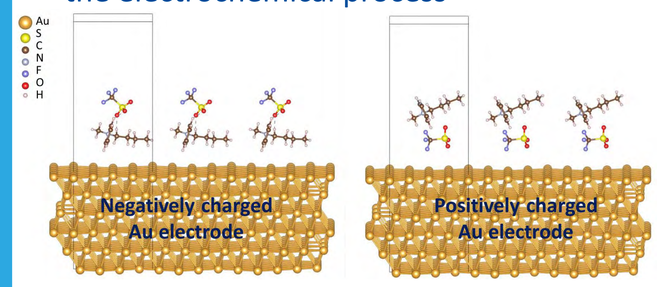

O. Clarke, A. Rowley, R. Heft, E. Engmann, M. Li, K. Sharmistha, R. Fox, I. Burgess and A. Atifi*

**Contact: abderrahman.atifi@inl.gov*

Project Number: 22A1059-040FP LRS Number: INL/EXP-23-74221

Work supported through the INL Laboratory Directed Research & Development (LDRD) Program under DOE Idaho Operations Office Contract DE-AC07-05ID14517."

New capability at Idaho National Laboratory for studying transuranic elements

Intrinsic Bonding and Reactivity of Actinide Clusters

PRESENTER: **Christopher Zarzana**

BACKGROUND: The purpose of this project is to develop new capability to study transuranic elements, increasing our understanding of chemical bond formation at the far edges of the periodic table. This is critical for solving technical challenges such as development of advanced nuclear fuel cycles and efficient rare earth separations, as well as a broader understanding of bonding across the entire periodic table.

RESULTS

- Established the capability at INL to study gas-phase complexes containing transuranic atoms.
  - One of only three instruments in the world
- Spectra collected using approximately 500 ng (~0.2 µCi) of ^{243}Am. We believe we can cut that amount down by at least a factor of 10, decreasing the radiolytic hazards and expanding the envelope of transuranics that can be investigated.

Approach:

- Atmospheric pressure ionization mass spectrometry can form clusters containing actinide atoms from extremely small quantities of radioactive material
- Metal-ligand interaction is probed in the gas phase, revealing intrinsic behavior

First spectra of transuranic cluster ions at INL

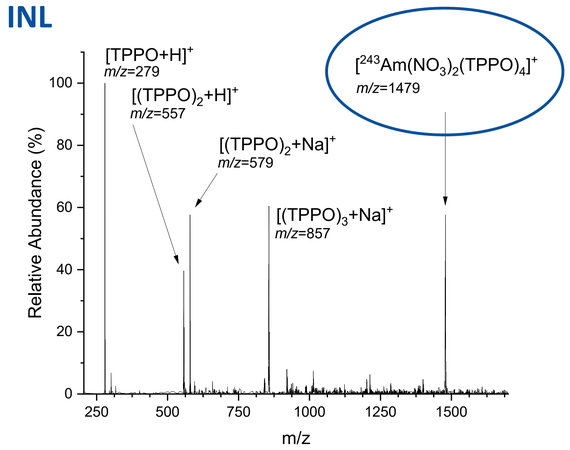

TPPO=triphenyphosphine oxide

Quantum chemistry calculations are underway to understand electronic structure

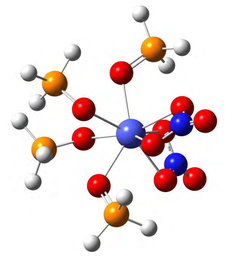

Zarzana, Christopher; Pilgrim, Corey; Kim, JungSoo; Hodges, Brittany

Project Number: 21A1057-017FP LRS Number: INL/EXP-23-74184

Work supported through the INL Laboratory Directed Research & Development (LDRD) Program under DOE Idaho Operations Office Contract DE-AC07-05ID14517."

Title: Development, Characterization, and Testing of Solid-State Electrolytes for Batteries

Presenter:
Corey Efaw

BACKGROUND: Batteries are needed to support the decarbonization movement, especially in the transportation sector (16.2% of all GHG emissions).[1] Lithium metal, solid-state batteries, could address many of the barriers seen in traditional Li-ion, liquid battery chemistries. In this work, ***sulfide-based solid-state electrolytes*** are synthesized through ***dry ball-milling*** and examined through various forms of characterization, to better understand the impact of synthesis parameters on make-up and performance.

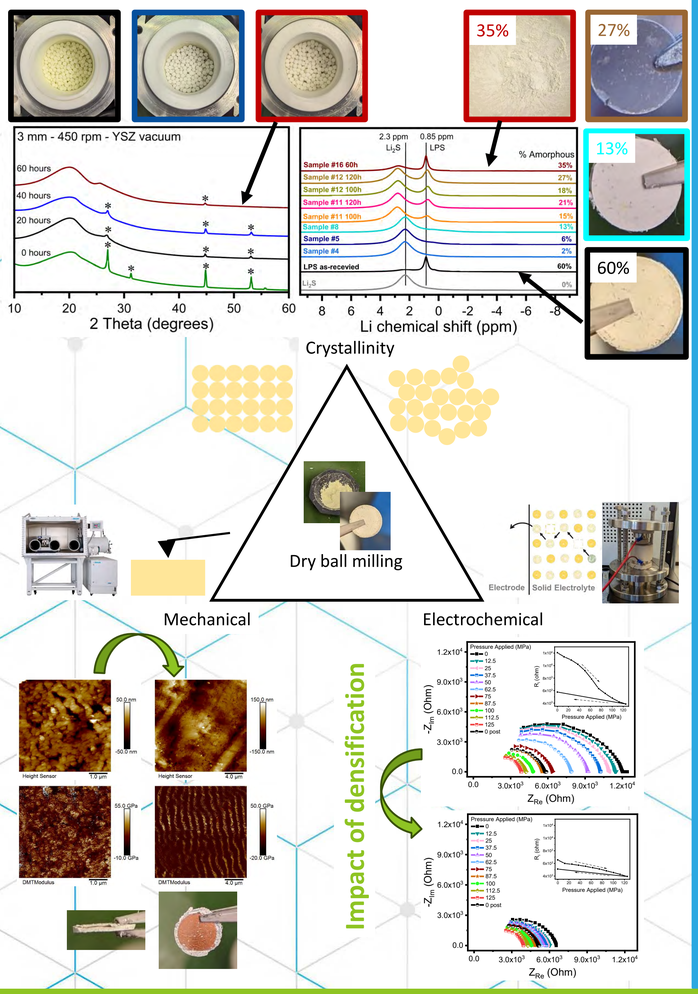

Literature is inconsistent to provide sufficient information on dry ball milling of solid-state electrolytes.

x - not documented in text

				Milling Media					Grinding Jar		Milling Details						
DOI	Year	mol ratio Li_2S:P_2S_5	Total active mass (g)	Material	Size(s)	Appx. Mass (g)	Count	Media: active (g:g)	Material	Size (mL)	RPM	Time (hr)	Milling Interval	Hand Milling	Jar Cleaning	Amorphous vs. Crystalline	Notes on Water Prevention
10.1111/j.1151-2916.2001.tb00685.x	2001	75:25	0.5-1	Alumina	10 mm	20	10	10-20	Alumina	45	370	20	Continuous	Y before	x	Amorphous	Milling in a glovebox
10.1016/j.elecom.2009.07.028	2009	70-80% Li_2S	1	ZrO_2	12 & 15 mm	15	1 each	x	ZrO_2	vial (Spex)	x	20	Continuous	x	x	Glass	Milling in a glovebox
10.1016/j.elecom.2009.07.028	2009	70-80% Li_2S	1	ZrO_2	12 & 15 mm	15	1 each	x	ZrO_2	vial (Spex)	x	20	30 min ON, 30 min OFF	x	x	Glass	Milling in a glovebox
10.1039/c0jm01090a	2011	80:20	x	ZrO_2	5 mm	60	160	x	ZrO_2	45	500	20	x	x	x	"Almost amorphous"	x
10.1016/j.ssi.2010.10.013	2011	67-80% Li_2S	x	ZrO_2	4 mm	120	500	x	ZrO_2	45	510	8-24	x	x	x	Glass & glass-ceramic	Dry Ar atmosphere
10.1038/srep02261	2013	75:25	x	ZrO_2	4 mm	120	500	x	ZrO_2	45	510	10	x	Y before	x	Amorphous	Dry Ar atmosphere
10.1016/j.jpowsour.2015.10.040	2015	75:25	1	ZrO_2	4 mm	120	500	x	ZrO_2	45	510	45	x	x	x	Unconfirmed	x
10.1038/nenergy.2016.30	2016	77:23	x	x	x	x	x	x	x	x	x	120	x	x	x	Crystalline	Milling in a glovebox
10.1038/srep21302	2016	67-75% Li_2S	x	ZrO_2	10 mm	32	10	x	ZrO_2	45	370	80	x	x	x	Mixture	Dry Ar atmosphere
10.1016/j.ssi.2015.11.034	2016	70:30	x	ZrO_2	3 mm	x	x	x	ZrO_2	80	510	144	10 min ON, 20 min OFF	Y, every 8h	x		Milling in a glovebox
10.1039/c7ta06067j	2017	50-75% Li_2S	5	ZrO_2	3 mm	110	x	22	ZrO_2	45	510	100	5 min ON, 15 min OFF	x	x	Amorphous below 75mol% Li2S	Milling in a glovebox
10.1149/2.1831712jes	2017	75:25	x	ZrO_2	4 mm	120	500	x	ZrO_2	45	510	10	x	x	x	Glassy	x
10.1038/s41467-018-04762-z	2018	77.5:22.5	x	x	x	x	x	x	Stainless Steel	500	x	20	x	x	x		x
10.1021/acs.jpcc.9b01425	2019	75:25	4	ZrO_2	3 mm	8.5	x	25	ZrO_2	45	510	117	5 min ON, 15 min OFF	x	x	Amorphous	Dry Ar atmosphere
10.1002/aenm.202101111	2021	75:25	x	ZrO_2	10 mm	36	12	x	ZrO_2	x	510	20	15 min ON, 15 min OFF	Y before	x	Crystalline	Sealed with parafilm & tape
10.1039/d1ta02754a	2021	75:25	2-5.2	ZrO_2	5 or 10 mm	32-64	x	6-16	ZrO_2	45	350-510	15-80	0-5 min OFF/hr	Varied	Varied	Amorphous	Screw-top clamp for sealing
10.1021/acsaem.0c02771	2021	75:25	x	x	x	x	x	x	ZrO_2	45	600	10	x	x	x		Milling in a glovebox
This work	22-23	75:25	2	YSZ	1.2-10 mm	20-70	varied	8-24	YSZ or Teflon	45-500	370-850	10-120	Varied	Varied	Varied	Commonly crystalline	Tape or screw-top clamp

METHODS:

XRD & NMR – XRD provides a go/no-go for crystalline/amorphous presence. NMR is more quantitative.[2]

Pelletization – 4 metric ton loading done for multiple samples. As-received LPS resulted in lower density (~40±2%), in-house prepared LPS (highly crystalline) samples had much higher density upon pelletization (>60%).

Mechanical testing (AFM – QNM) – Only as-received sample analyzed, both after pelletization and after testing at 1 metric ton load in a symmetric test with SS. Material density changed after operation at high pressure, but mechanical properties did not vary in range.

Electrochemical testing – Only as-received samples operated in the non-resistive regime. Electrochemical impedance spectroscopy (EIS) was used to measure SSE Bulk conductivity (R_b) with an ion-blocking electrodes (SS), while interfacial charge transfer (**R3**) is characterized with ion-conducting electrodes (Li). Cycling was run in a constant-current design, within a ± 1V range. EIS was measured after each cycle. Artificial solid-electrolyte interphases (SEIs) were tested against pure Li to observe interfacial charge transfer.

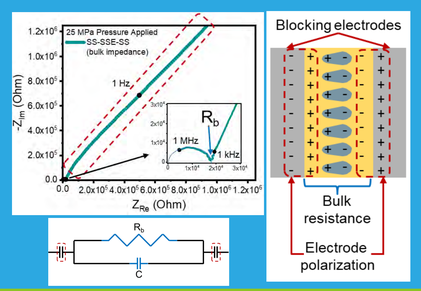

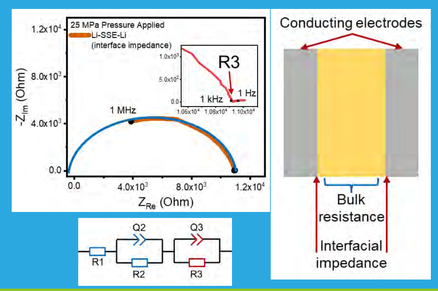

OTHER FINDINGS:

Milling parameters to consider:

- Milling rate
  - 370-540 rpm shows no clear trends
- Time
  - Extending time increases amorphous behavior
  - Extending time also increases “burn effect”
- Media
  - Benefit to use same media as container (YSZ)
  - Size doesn’t reveal any trends…particle size TBD
  - Number of media has no trends
- Container
  - Use of an isolation container is key to achieve higher amorphous content with less time milling
  - Small jar + large media = greater edge adhesion
- Cleaning
  - DMF cleaning + ethanol/DI rinse = reduced adhesion to edges & less flakes
  - Hand milling improves uniform powder size

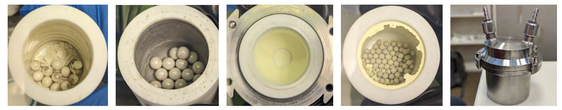

Cycle testing

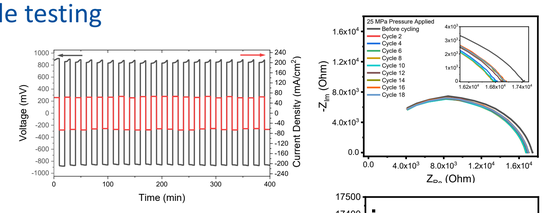

Bulk electrolyte testing

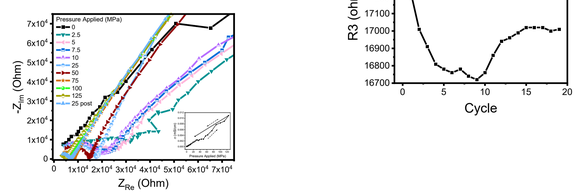

Artificial Solid-electrolyte interphase (SEI) testing

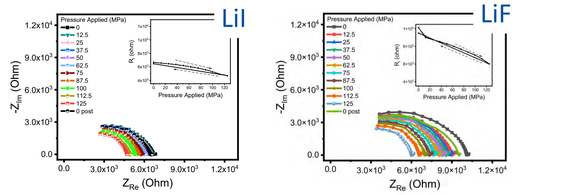

[1]OurWorldInData.org
[2]Mirmira et al, doi: 10.1039/d1ta02754a

Acknowledgments: Corey Pilgrim, Pete Barnes, Bor-Rong Chen, Bumjun Park, Bin Li, Eric Dufek, Josh Gomez, Dong Ding (INL), Paul Davis, Elton Graugnard, JD Hues (Boise State)

Project Number: 22P1066-006FP

LRS Number: INL/EXP-23-74155

Work supported through the INL Laboratory Directed Research & Development (LDRD) Program under DOE Idaho Operations Office Contract DE-AC07-05ID14517."

Transport properties of lanthanides strongly influenced by ligand addition

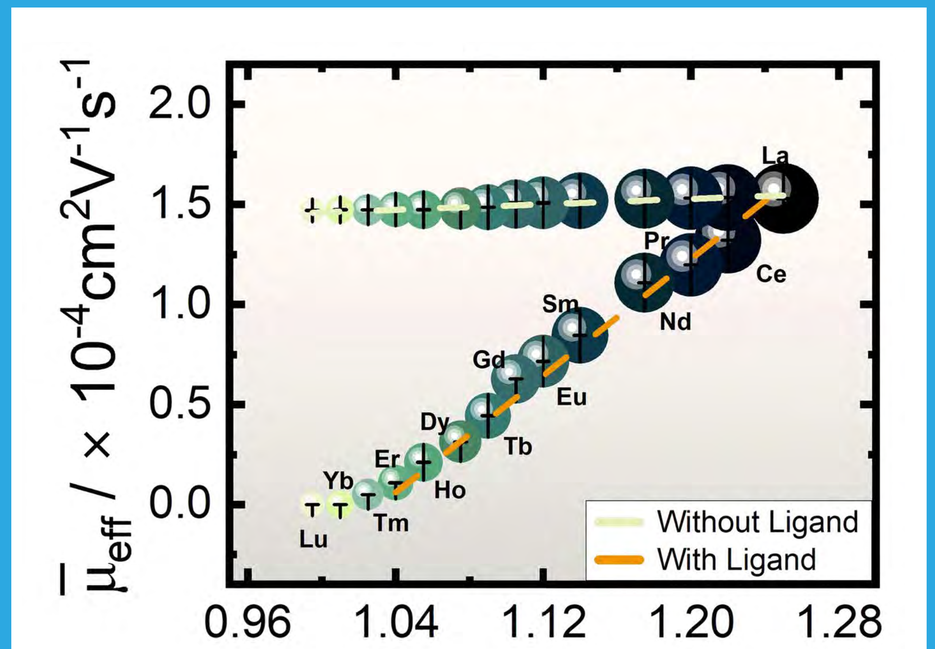

Chloe Tolbert, Swapnil Bamane, Gorakh Pawar, Mary Case, Caleb Hill, Robert Fox

Method

Ligands **alter** the chemical environment of lanthanides.

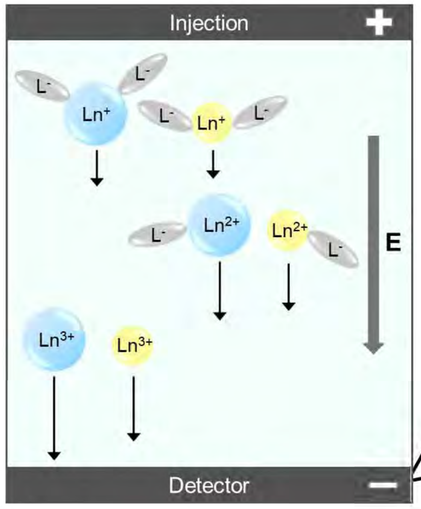

Changes in transport properties allow for **enhanced** separations!

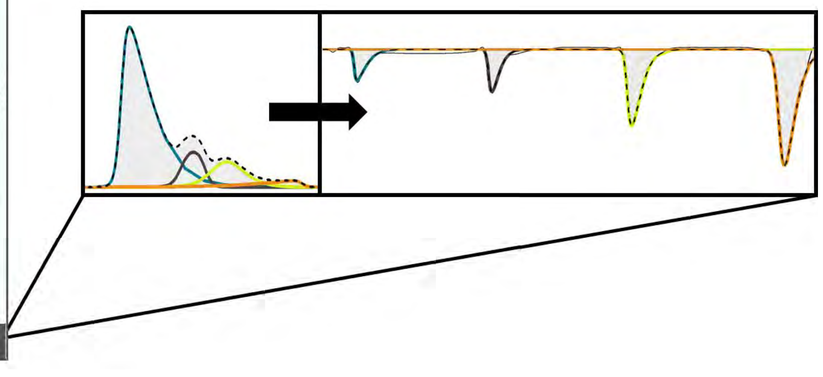

Preferential coordination is responsible for enhanced light/heavy separations.

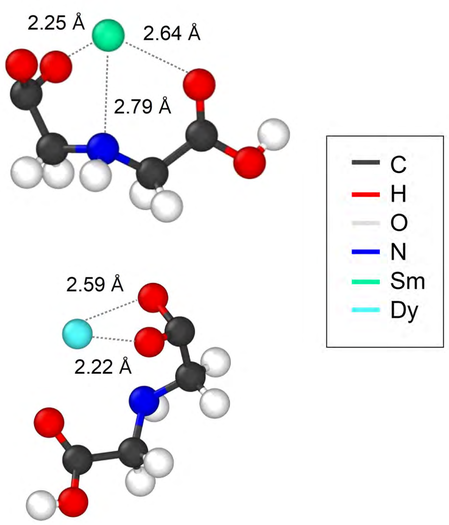

Baseline resolution achieved between 10/13 lanthanides *via* ligand competition.

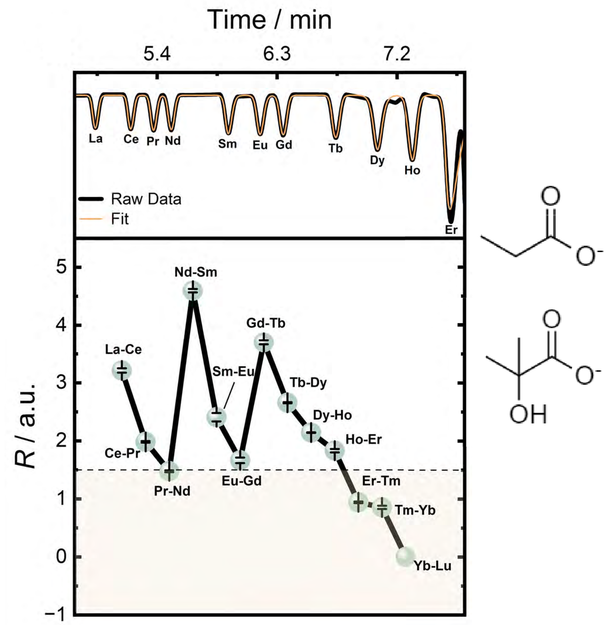

Project Number: 22A1059-096FP

LRS Number: INL/MIS-23-74214

Work supported through the INL Laboratory Directed Research & Development (LDRD) Program under DOE Idaho Operations Office Contract DE-AC07-05ID14517."

Condensed Matter Physics and Materials Science

Kaustubh Bawane	Phase Stability of Yttrium-Titanium Oxides
Kris Gofryk	Electronic and transport properties of single-crystalline neptunium telluride
Michael Benson	Investigation of stability in the uranium-zirconium intermetallic compound
Mukesh Bachhav	Thermal diffusivity measurement in nano-crystalline oxides using laser assisted atom probe tomography
Shuxiang Zhou	Point defects in uranium dioxide by density functional theory Hubbard model: defect local environment and occupation matrix control

Work supported through the INL Laboratory Directed Research & Development (LDRD) Program under DOE Idaho Operations Office Contract DE-AC07-05ID14517."

Phase Stability of Yttrium Titanium Oxides

Xiaofei Pu, Eitan Hershkovitz, Fidelma DiLemma, **Kaustubh Bawane**, Honggyu Kim, Lingfeng He

Background

YTO – a critical nuclear material

- Nanoparticles in ODS steels
- Rare-earth titanate pyrochlore for nuclear waste immobilization
- Important to study phase transitions in extreme conditions

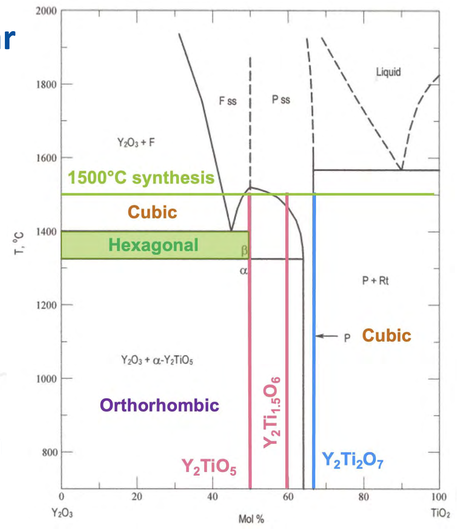

Methods

Materials (powder and bulk) Y_2TiO_5, $Y_2Ti_{1.5}O_6$, $Y_2Ti_2O_7$

In-situ high-temperature XRD up to 1200°C to study phase and microstrain evolution

Ex-situ and In-situ TEM up to 1200°C – atomic scale imaging of phases and defects

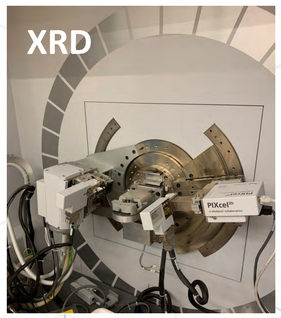

We studied phases in YTO using in-situ XRD and TEM techniques. TEM images of hexagonal phase in Y_2TiO_5 were recorded for the first time!

In-situ heating of Y_2TiO_5 in XRD - No phase transition up to 1200°C

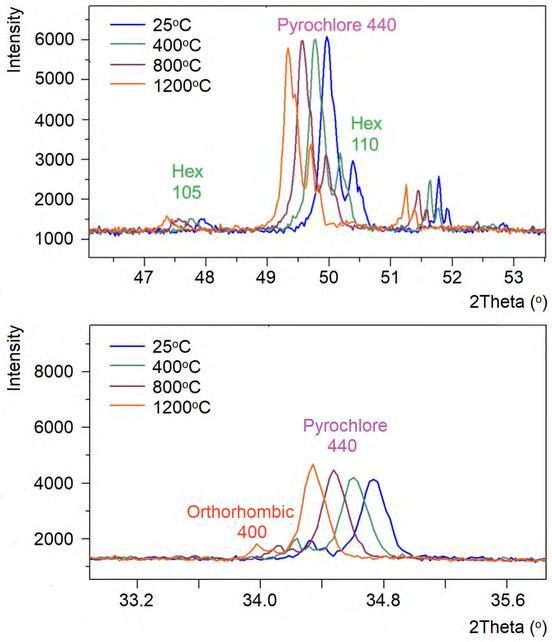

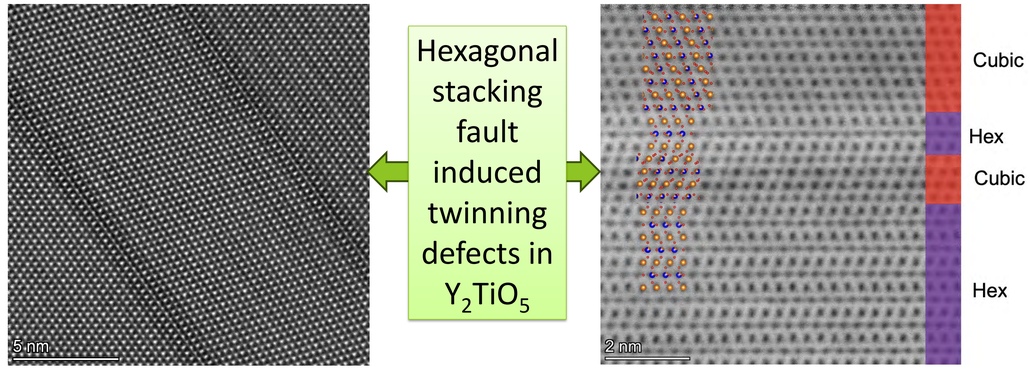

Cubic phase shows mixed pyrochlore and fluorite structures – confirmed by 4D STEM mapping

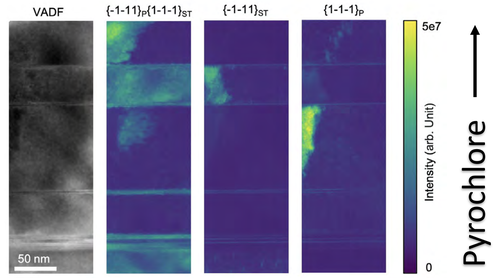

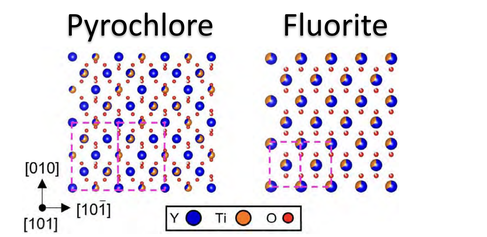

Pyrochlore is 2x2 supercell of Fluorite with additional cation ordering

EBSD Phase analysis of Y_2TiO_5 showing increase in hexagonal phase after heating

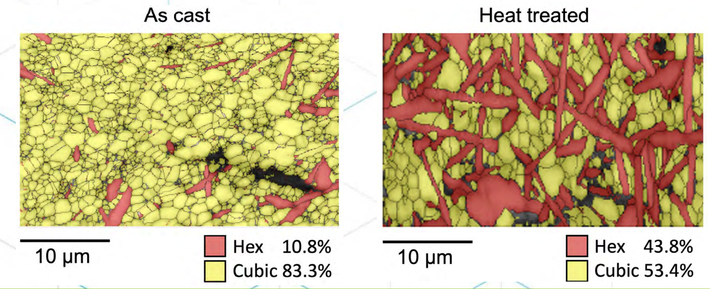

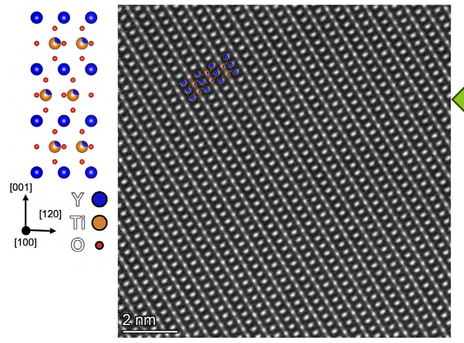

First ever HAADF-STEM image of hexagonal phase in Y_2TiO_5

Project Number: 22P1065-024FP LRS Number: INL/MIS-23-74287

Work supported through the INL Laboratory Directed Research & Development (LDRD) Program under DOE Idaho Operations Office Contract DE-AC07-05ID14517."

www.inl.gov

Battelle Energy Alliance manages INL for the U.S. Department of Energy's Office of Nuclear Energy

Idaho National Laboratory

Narayan Paudel (co-PI),
Daniel Murray (co-PI),
and Krzysztof Gofryk (PI)

Electronic and transport properties of single-crystalline neptunium telluride

Background

Binary chalcogenides occur abundantly in nature, have a variety of applications, and exhibit many novel behaviors. For instance, UTe_2 was recently shown to exhibit an unprecedented electronic phase diagram with unconventional superconductivity, enormous upper critical fields, possible spin triplet pairing, and non-trivial electronic structure. These diverse behaviors motivated us to investigate the actinide analogue $NpTe_2$.

Methods

Single crystal synthesis - iodine vapor transport with elemental starting components (neptunium metal 99.9%, tellurium 99.999%, and iodine 99.999%)

Characterization – single crystal diffraction, scanning electron microscope, dispersive X-ray spectroscopy,

Low temperature Magnetic and transport measurements – Quantum Design MPMS and PPMS, plasma Focuses Ion Beam micromachining

W. L. Nelson, A. S. Jayasinghe, Joseph M. Sperling, N. Beck, Todd N. Poe, D. Murray, N. Poudel, R. Kennedy, S. Latturner, Thomas E. Albrecht-Schonzart, Jianxin Zhu, K. Gofryk, and R. E. Baumbach
"*Kondo Lattice Semimetallic Behavior in $NpTe_{1.75}$ single crystals*"
- in preparation (intended for Phys. Rev. Letters)

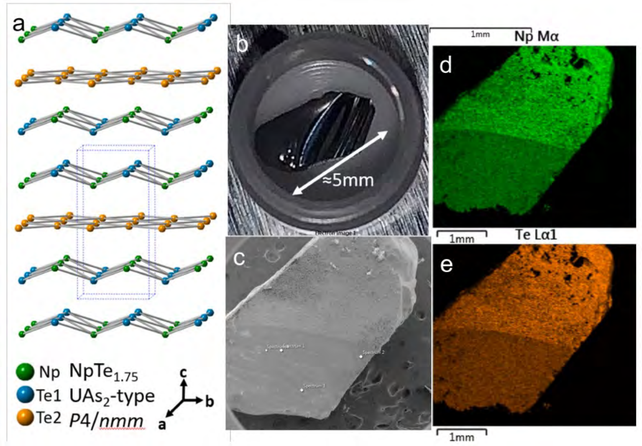

	$NpTe_{1.75}$
Structure Type	UAs_2
Space Group	$P4/nmm$
Molar Mass (g/mol)	460.3
Density (g/cm^3)	8.934
Lattice Constants (Å)	a = 4.3559(5) b = 4.3559(5) c = 9.0167(11)
Volume (Å^3)	171.08
Z	1
μ(mm^{-1})	44.684
F(000)	367.9
Theta (max) ^{o}	30.458
h,k,l (max)	6, 6, 12
Reflections	R1 = 0.0384(189) wR2 = 0.0856(190)

- $NpTe_{1.75}$ single crystals
- Tetragonal, UAs_2-type, s.g. P4/nmm

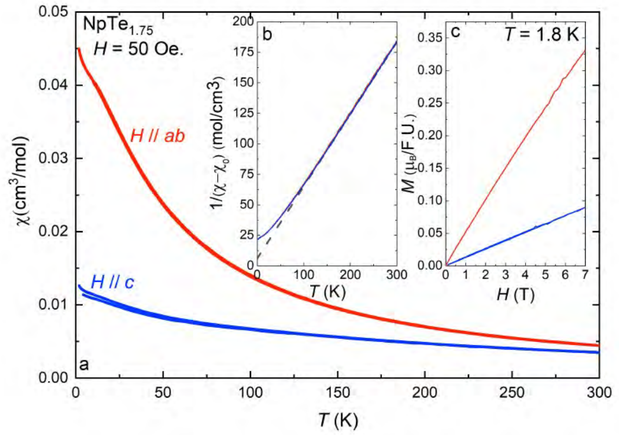

- Curie Weiss Paramagnetic, Np^{4+}

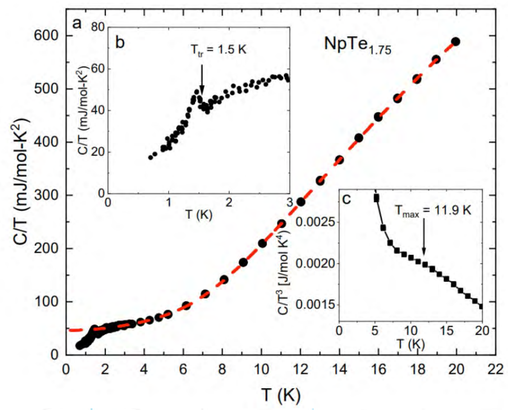

- Enhanced Sommerfeld coefficient,
  $-\gamma$ = 45 mJ/molK^2
- Transition at 1.5 K?

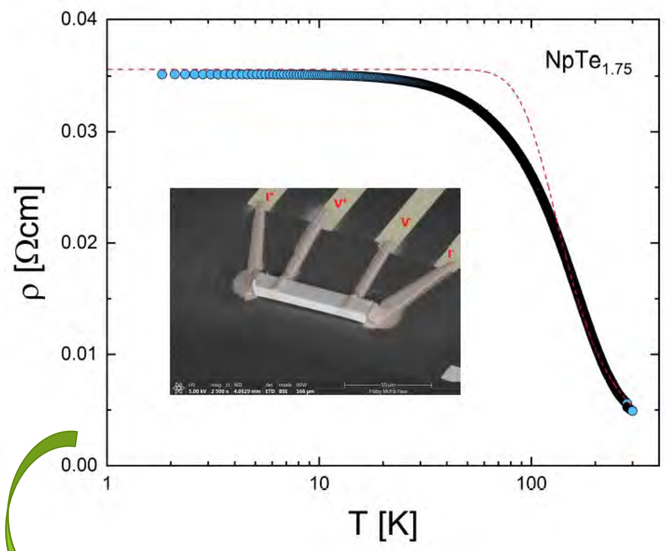

$$\frac{1}{\rho(T)} = \sigma_a + b\exp\left(\frac{-E_g}{k_B T}\right) \qquad E_g = 45 \text{ meV}$$

- Narrow gap semiconductor
- **Topological characteristics?**

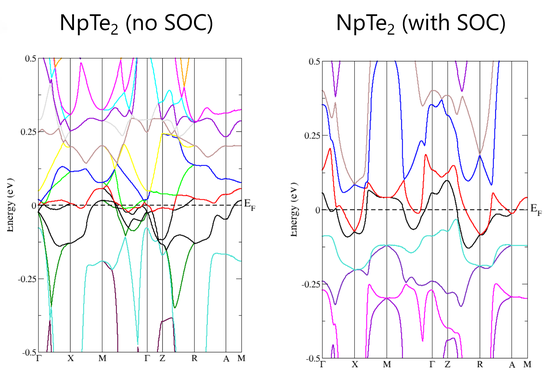

- Band inversion
- Gap opening
- **Non-trivial?**

Project Number: 22P1068-012FP
LRS Number: INL/MIS-23-74279
Work supported through the INL Laboratory Directed Research & Development (LDRD) Program under DOE Idaho Operations Office Contract DE-AC07-05ID14517."

Title: Investigation of Stability in the U-Zr Intermetallic Compound

PRESENTER: **Michael T. Benson**

BACKGROUND: The U-Zr phase diagram has been used to interpret the behavior of U-Zr fuels, in and out of the reactor, for over 60 years, but the phase diagram is incorrect.

METHODS: Samples of UZr_2 were annealed at 500°C while sealed in quartz tubes under vacuum. Samples characterized using scanning electron microscopy (SEM), transmission electron microscopy (TEM), X-ray diffraction (XRD), and atom probe tomography (APT). Density functional theory (DFT) calculations with the Perdew-Burke-Ernzerhof functional were performed. TEM and APT are ongoing now.

RESULTS: δ-UZr_2 is a long-lived metastable phase and should not be included in the U-Zr phase diagram. As-cast δ-UZr_2 (determined by XRD) decomposed into α-U and α-Zr after long annealing times. δ-UZr_2 is a long-lived metastable phase.

UZr_2 annealed for short time. Shown for comparison

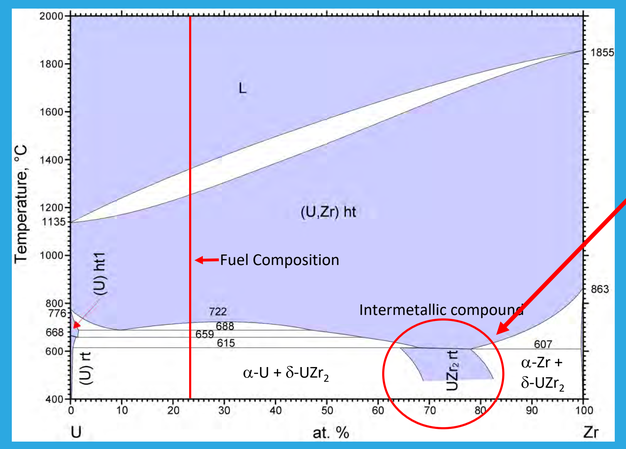

Indicates thermodynamically stable intermetallic phase

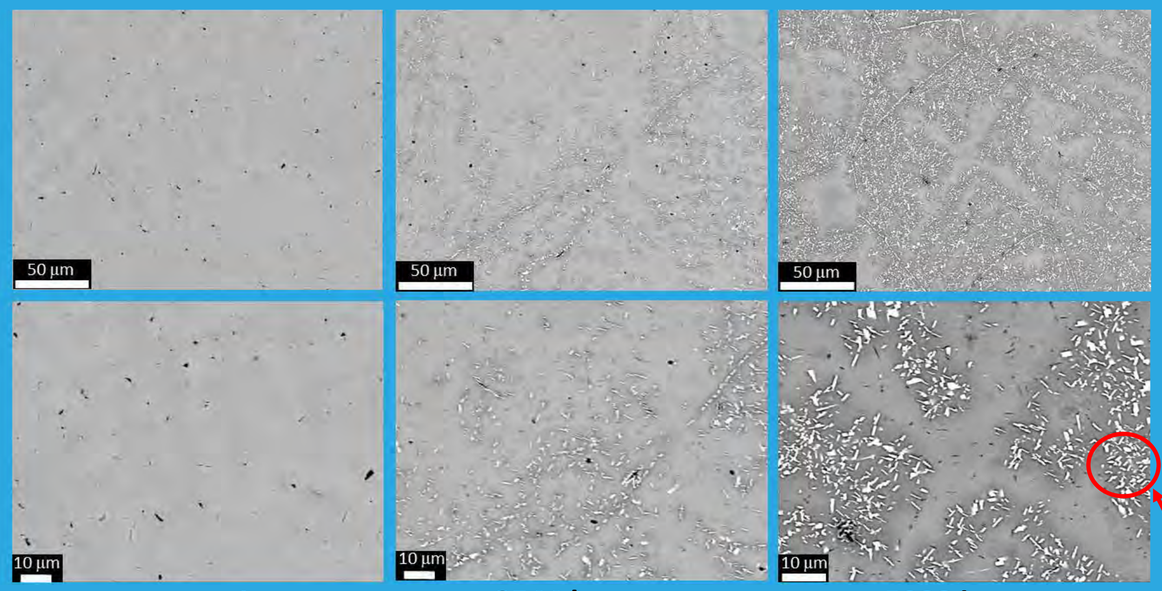

SEM images of UZr2 alloy, as-cast and after annealing

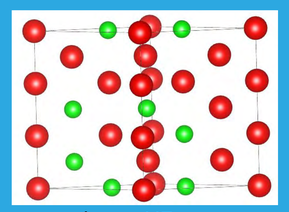

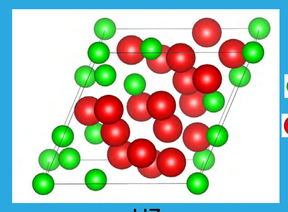

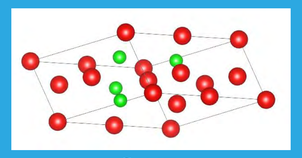

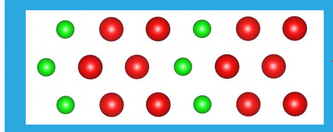

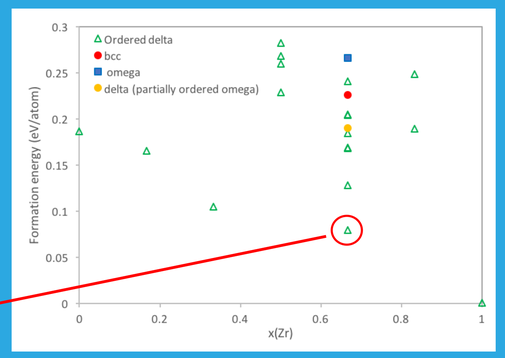

DFT calculations indicate most stable UZr_2 structure is ordered δ-UZr_2, a phase separated state. Onset of spinodal decomposition?

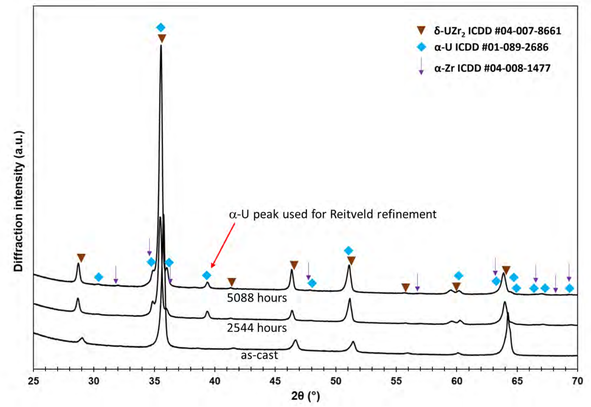

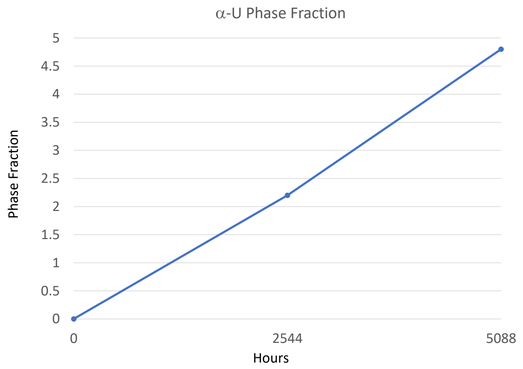

XRD results shown, with plotted α-U phase fraction

White precipitates are α-U. Black precipitates are α-Zr (can't be quantified due to peak overlap).

Michael Benson, Josh Zelina, Tiankai Yao, Chao Jiang, Mukesh Bachhav, Jennifer Watkins

Project Number: 22P1068-011FP LRS Number: INL/MIS-23-74042

Work supported through the INL Laboratory Directed Research & Development (LDRD) Program under DOE Idaho Operations Office Contract DE-AC07-05ID14517."

Adding another dimension to Atom Probe analysis: *Thermal diffusivity measurement of ceramic fuels at nanoscale*

What APT does well?

☑ 3D microstructure at sub-nanoscale

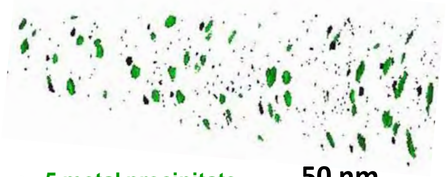

- 5 metal precipitate (Rh, Ru, Pd, Tc, Mo)
- Xe

50 nm

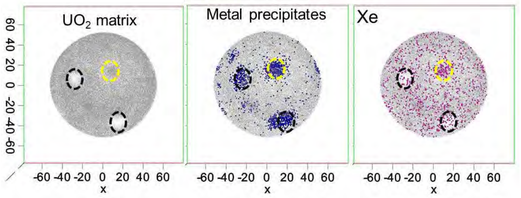

Fission product distribution in spent UO_2 ceramic fuel

☑ Quantitative chemical analysis at nanoscale

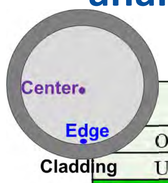

		Center	*Edge*
	O	66.01	65.45
	U	32.25	32.04
Solid solution		0.18	0.26
Metal precipitates		0.41	0.77
Volatile fission products		0.37	0.53
Oxide precipitates		0.20	0.42
Total fission products		1.16	1.98

Compositional analysis from UO_2 and fission products in spent fuel [1]

☑ Burnup and enrichment measurement in nuclear fuel

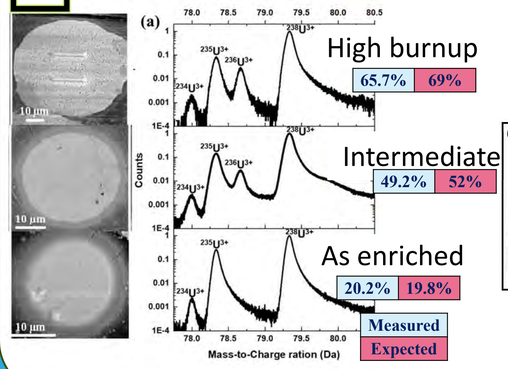

$$U-235\ Burnup=\frac{\left[\frac{U_{235}}{U_{total}}\right]_{BOL}-\left[\frac{U_{235}+U_{236}}{U_{total}+Pu_{total}}\right]_{EOL}}{\left[\frac{U_{235}}{U_{total}}\right]_{BOL}}$$

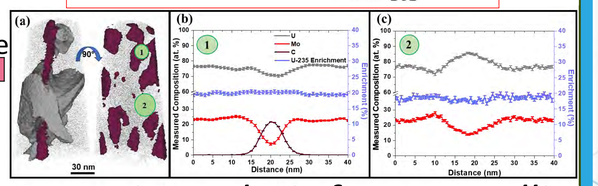

Isotopic analysis from metallic UMo fuel [2]

Mukesh Bachhav, Rahul Reddy Kancharla, Krzysztof Gofryk, Tsvetoslav Pavlov, Amrita Sen

Method: Thermal diffusivity assessment based on laser-tip interaction in Atom Probe Tomography (APT)

Laser locally "heats" nanometric tip during field evaporation process

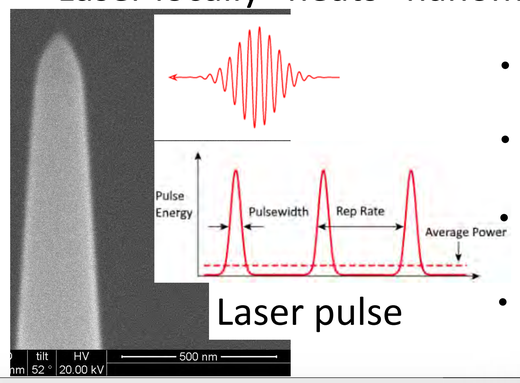

- **Field evaporation** process in APT $N_{ions}(t)=nexp(-\frac{Q}{k_BT_s(t)})$
- Thermal diffusion $\frac{\partial T}{\partial t}=D\ \frac{\partial^2 T}{\partial z^2}$
- **Modifield analytical solution** $T_s(t)=T_{max}\left(\frac{1}{\sqrt{1+\frac{tD}{\sigma^2}}}+\frac{f(E_p)}{\sqrt{1+\frac{tD}{\sigma^2}}}e^{\left(-\frac{z^2}{2\sigma^2\sqrt{1+\frac{tD}{\sigma^2}}}\right)}\right)$
- ***Temperature rise*** due to laser-tip interaction $T_{rise}=T_0+\alpha Ep$

[3]

Mass spectrum showing thermal tail with "hump" with change in laser energy for pristine ThO_2

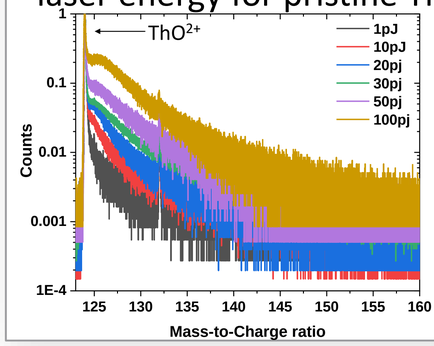

[4]

Mass spectrum for proton irradiated ThO_2 as a function of laser energy showing thermal tail

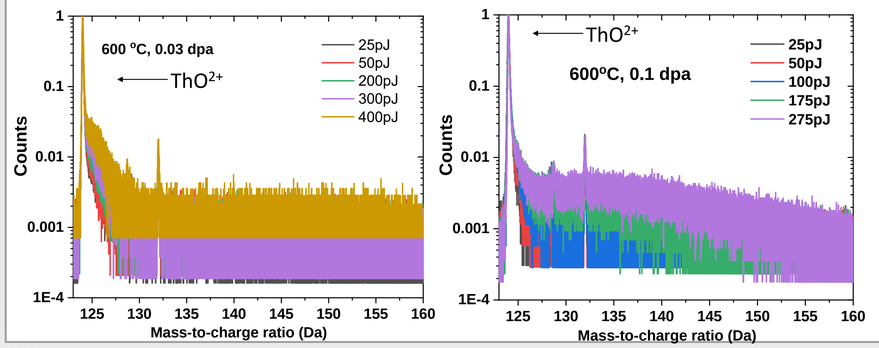

Thermal diffusivity measured on pristine and irradiated ThO_2 using spatial-domain thermoreflectance (SDTR)

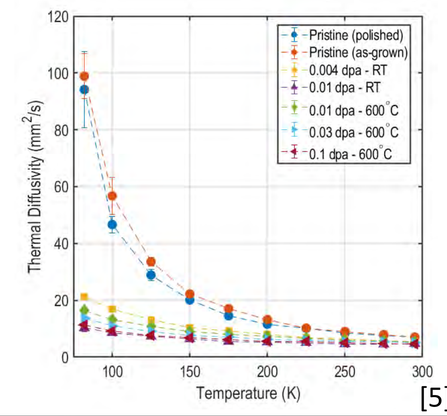

[5]

Thermal diffusivity measured by fitting experimental mass spectrum with analytical model developed using MATLAB for different laser energy

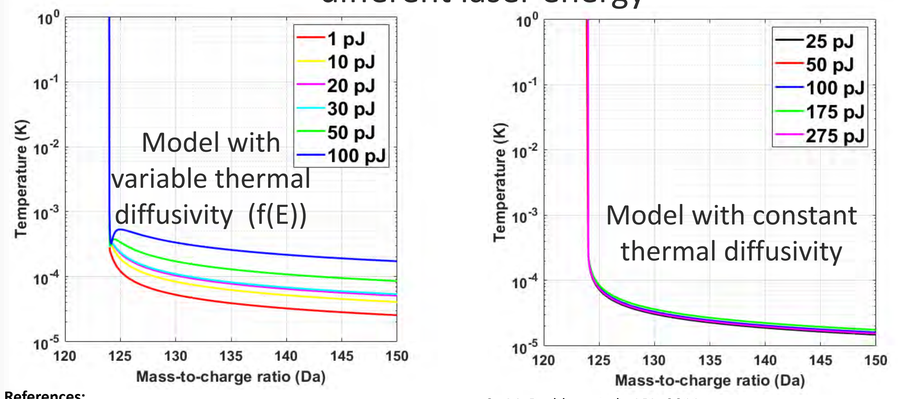

References:

1. A. Ditter, M. Bachhav et al. J of Synchrotron radiation, 2021
2. M. Bachhav et al. JNM, 2020
3. M. Bachhav et al. APL, 2011
4. A. Sen, M. Bachhav, et al. Ultramicroscopy, 2021
5. C. Dennett, et al. Acta Mat, 2021

Project Number: 22P1071-028FP

LRS Number: INL/EXP-23-74327

Work supported through the INL Laboratory Directed Research & Development (LDRD) Program under DOE Idaho Operations Office Contract DE-AC07-05ID14517."

Point defects in UO_2 by DFT+U: defect local environment and occupation matrix control

Background

Defects are critical to thermal and mechanical behavior of nuclear fuel materials, like UO_2, under irradiation. While first-principles calculations bring up a method to compute the defect formation energy, it is still a technical challenge to model Mott insulators, due to complex interplay between Mott physics, magnetism, and spin-orbit coupling (SOC).
In fact, the intrinsic defects have only been computed in UO_2 using 1k antiferromagnetic (AFM) structure without SOC. Here, we develop a method to compute the defect formation energy under different magnetic orderings with SOC and further reveal their effects.

Methods

1. Density functional theory and the Hubbard U approximation (DFT+U) at 0K
2. *f*-orbital single-atom occupation matrix control (OMC)
3. 2 (3) different magnetic orderings are applied without (with) SOC: ferromagnetic, 1k AFM, and 3k AFM (only with SOC).

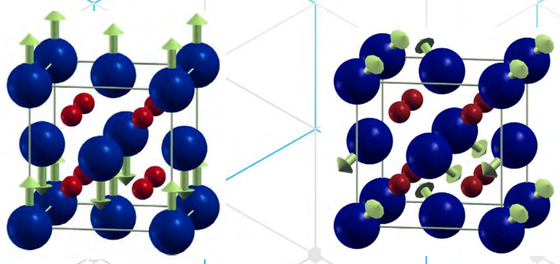

1k AFM (left) and 3k AFM (right) structures
From J. Condens. Matter Phys.25, 333201 (2013).

The magnetic ordering and spin-orbit coupling have substantial effects on defect formation energy in UO_2.

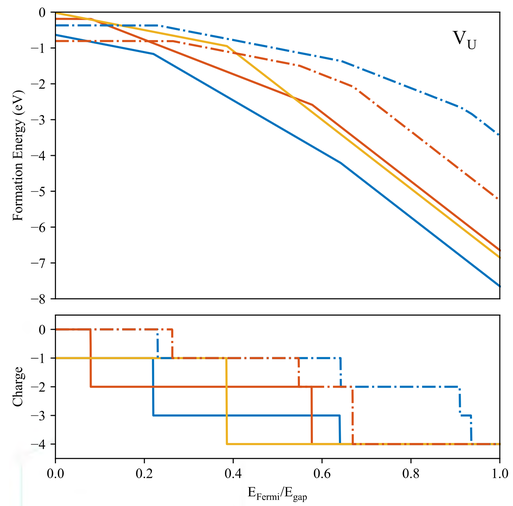

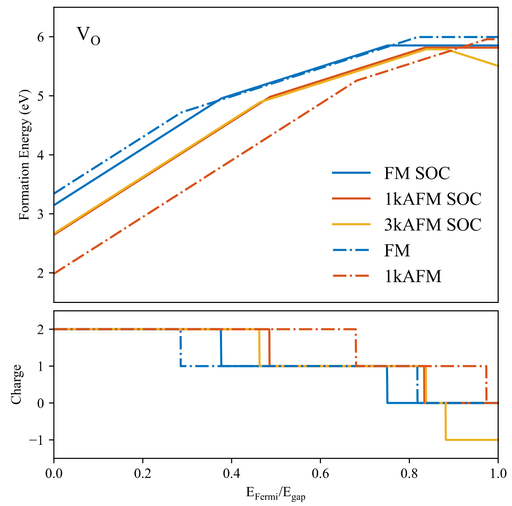

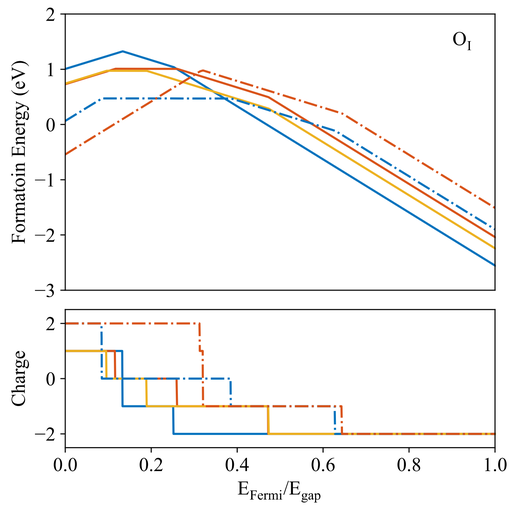

The difference in defect formation energy is induced by different mechanism of U atom distortion:

1. Different magnetic ordering changes the position of U^{5+} or U^{3+} cations;
2. Under SOC, rather than the presence of U^{5+} or U^{3+} cations, U tends to rotate magnetic moments;
3. 1kAFM SOC can serve as a good approximation for the noncollinear 3kAFM SOC structure.

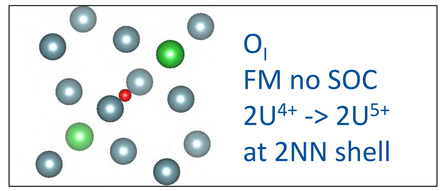

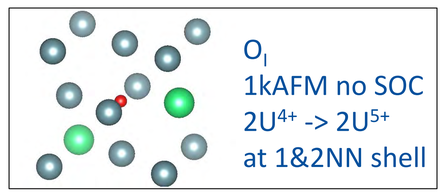

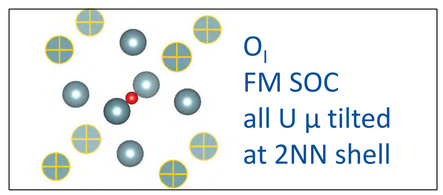

Shuxiang Zhou and Chao Jiang

Project Number: 22P1066-001FP LRS Number: INL/MIS-23-74237

Work supported through the INL Laboratory Directed Research & Development (LDRD) Program under DOE Idaho Operations Office Contract DE-AC07-05ID14517."